Solvation Dynamics by Coherence Period Resolved Transient Grating

ARTICLE *in* THE JOURNAL OF PHYSICAL CHEMISTRY A · FEBRUARY 2011

Impact Factor: 2.69 · DOI: 10.1021/jp108495t · Source: PubMed

3 AUTHORS, INCLUDING:

Taiha Joo
Pohang University of Science and Technology
131 PUBLICATIONS **4,041** CITATIONS

THE JOURNAL OF PHYSICAL CHEMISTRY A

ARTICLE

pubs.acs.org/JPCA

Solvation Dynamics by Coherence Period Resolved Transient Grating

Sohyun Park, June-Sik Park,† and Taiha Joo*

Department of Chemistry, Pohang University of Science and Technology (POSTECH), Pohang, 790-784, Korea

ABSTRACT: We report a third-order nonlinear time-domain method, coherence period (τ) resolved transient grating (TRTG), that gives accurate solvation dynamics free from population relaxation in a short data acquisition time. The validity of TRTG is established by theory and experiment. The TRTG signal is shown to follow the transition frequency correlation function by an analytic expression based on the response function theory for delta function pulses and by model numerical calculations including finite pulse durations. TRTG is demonstrated for two cyanine dyes IR144 and IR125 in methanol by using a diffractive-optics based four wave mixing apparatus. Solvation dynamics in methanol obtained from the TRTG are consistent with those reported previously confirming the validity of TRTG.

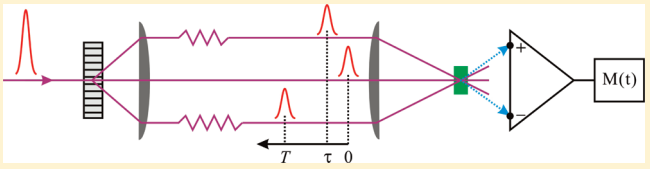

INTRODUCTION

Interaction of a solute with bath degrees of freedom is a basic property that lies behind most of the physical and chemical processes in condensed phases including chemical reactions as well as the spectral line broadening. The interaction is determined by the spectral density of the bath weighted by the coupling strength of each bath mode to a relevant variable. For an electronic transition of a dye molecule in liquid, the transition frequency is modulated by the interaction of the molecule with the bath, where the bath includes intramolecular as well as intermolecular. The interaction, which is the solvation dynamics for this system, is manifested in the line broadening and time-dependent shifts of the absorption and emission spectra.[1−4] As the spectral density of a simple liquid usually starts from near zero and stretches to rather high frequency showing a maxima around 50−100 cm^{-1},[5−7] the time scale of the interaction spans over a wide range from less than 100 fs to nanoseconds.

The solvation dynamics can be represented by the Stokes shift function $S(t)$ acquired from the time-dependent fluorescence spectra[8]

$$S(t) = \frac{\overline{\omega}(t) - \overline{\omega}(\infty)}{\overline{\omega}(0) - \overline{\omega}(\infty)} \quad (1)$$

where $\overline{\omega}(t)$ is the characteristic frequency of the fluorescence spectrum such as the first moment at time t. Through the fluctuation−dissipation relation, solvation dynamics can be equally described by the transition frequency correlation function[1,9]

$$M(t) = \frac{\langle \Delta\omega(t)\, \Delta\omega(0) \rangle}{\langle \Delta\omega^2 \rangle} \quad (2)$$

where $\Delta\omega(t) = \omega(t) - \langle\omega_{eg}\rangle$. Here $\langle\omega_{eg}\rangle$ is the average transition frequency of a two-level system, $\omega(t)$ is the transition frequency at time t, and the brackets denote an ensemble average.

Several third-order nonlinear time-domain methods such as the three pulse photon echo peak shifts (3PEPS), transient absorption (TA), and transient grating (TG) as well as time-resolved fluorescence have been used to obtain the detailed information on the coupling strengths and the time scales of the solvation dynamics.[9−16] In TG, two concurrent pump pulses, whose wave vectors are $\mathbf{k}_1$ and $\mathbf{k}_2$, generate a transient grating in the sample, and a time delayed third pulse $\mathbf{k}_3$ is diffracted off the grating. The signal into the phase matching direction $-\mathbf{k}_1+\mathbf{k}_2+\mathbf{k}_3$ (or $+\mathbf{k}_1-\mathbf{k}_2+\mathbf{k}_3$) is measured while scanning the time delay. Since the transient grating is destroyed by spectral diffusion and spatial diffusion as well as population relaxation, a TG signal is sensitive to both population relaxation and solvation dynamics,[17] although it may be nontrivial to extract solvation dynamics (spectral diffusion) from a TG signal free from population relaxation and other dynamics that diminish the TG intensity. In 3PEPS, a peak shift of a photon echo signal from time zero is recorded accurately in a three pulse stimulated photon echo experiment as a function of the population period by measuring the signals at the two phase-matching directions $-\mathbf{k}_1+\mathbf{k}_2+\mathbf{k}_3$ and $+\mathbf{k}_1-\mathbf{k}_2+\mathbf{k}_3$.[9,14,18] It has been well established by theory and experiment that 3PEPS follows $M(t)$ closely.[9] Since 3PEPS measures the peak shift, not intensity, it is free from population relaxation and spatial diffusion dynamics. In addition, inhomogeneity of the system with a time scale longer than the lifetime of the probe molecule can be measured unambiguously.[19] Although $M(t)$ can be best determined by 3PEPS, it requires a long acquisition time, because two-dimensional scans with respect to the coherence and population periods are needed.

In this paper, we report a four wave mixing scheme, τ-resolved transient grating (TRTG), that gives accurate solvation dynamics free from population relaxation with a short acquisition time. It is a mix of TG and 3PEPS experiments; population time T (see Figure 1 for pulse ordering and time conventions) is scanned as

Special Issue: Graham R. Fleming Festschrift

Received: September 6, 2010
Revised: January 17, 2011
Published: February 10, 2011

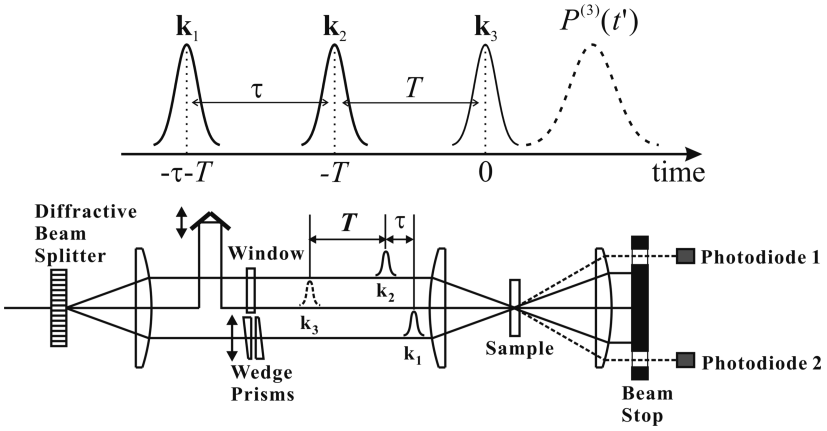

Figure 1. (Top) Time ordering of pulse sequences and notations for the time intervals. $P^{(3)}(t')$ is the third-order polarization generated by the three field-matter interactions. (Bottom) Schematic of the diffractive beam splitter based TRTG apparatus.

in a TG while the electronic coherence time (τ) is fixed at a small nonzero value,[17] and the two signals into the phase matching directions $-\mathbf{k}_1+\mathbf{k}_2+\mathbf{k}_3$ and $+\mathbf{k}_1-\mathbf{k}_2+\mathbf{k}_3$ are measured simultaneously as in a 3PEPS. We define the TRTG from the intensities of the two signals at $-\mathbf{k}_1+\mathbf{k}_2+\mathbf{k}_3$ and $+\mathbf{k}_1-\mathbf{k}_2+\mathbf{k}_3$. We will then show by theory and experiment that a TRTG reproduces $M(t)$ rather closely.

EXPERIMENT

The light source was a home-built cavity-dumped Kerr lens mode-locked Ti:sapphire laser generating 20 fs pulses at 780 nm. To avoid the thermal grating effect and other power-induced artifacts, pulse energies were attenuated to 1 nJ at a repetition rate of 150 kHz. The laser spectrum was nearly a Gaussian with a bandwidth of ~50 nm full width at half-maximum.

Schematic of the TRTG apparatus based on a diffractive beam splitter is shown in Figure 1, which is nearly the same as the 3PEPS setup reported previously.[19] The laser output passes through a pair of fused silica prisms to compensate the group velocity dispersion (GVD). The laser beam was focused onto a fused silica diffractive beam splitter (DBS) by a 30 cm focal length lens to generate a triplet of identical pulses at the diffraction orders of 0 and ±1. The DBS generates tilted phase front and allows the femtosecond pulses to overlap over the full aperture while preserving pulse duration.[20,21] Two first-order diffracted beams served as pump pulses $\mathbf{k}_1$ and $\mathbf{k}_2$, while the zero-order diffraction was used as a probe pulse $\mathbf{k}_3$. The $\mathbf{k}_1$ beam passes through a pair of BK7 wedge prisms with center thicknesses of 3.8 mm and wedge angles of 3.86°. One of the wedge prisms was mounted on a motorized translational stage with a resolution of 0.055 μm to control the amount of glass in the beam path, which in turn controls the optical delay τ between $\mathbf{k}_1$ and $\mathbf{k}_2$. In this way, τ can be controlled accurately at a time resolution of 6.6 as.[17] A 6.35 mm thick BK7 window was inserted in each beam pass of $\mathbf{k}_2$ and $\mathbf{k}_3$ to compensate the GVD. The moving wedge was positioned in such a way that the amount of glasses for $\mathbf{k}_1$ and $\mathbf{k}_2$ are the same at $\tau = 0$. The resolution and stability of the time delay, especially the τ delay, was confirmed by optical interferometry by collinearly propagating a He−Ne laser beam. The setup maintained interferometric accuracy for several hours without any feedback. The three pulses forming an isosceles were focused on a 200 μm path length fused silica flow cell containing sample solutions. Two signals into the phase matching directions $-\mathbf{k}_1+\mathbf{k}_2+\mathbf{k}_3$ and $+\mathbf{k}_1-\mathbf{k}_2+\mathbf{k}_3$, defined as I_R and I_{NR}, respectively, were measured simultaneously, and TRTG was defined as $(I_R - I_{NR})/I_{NR}$.

Steady state fluorescence spectra of the samples were measured with a He−Ne laser as an excitation source. Fluorescence collection was done at perpendicular to the beam path with a spectrometer equipped a CCD array detector.

IR144 and IR125 from Exciton Co. and methanol from Aldrich were used without further purification. Concentration of each solution was adjusted to give an absorbance of 0.3 at the absorption maximum, which resulted in a dye concentration of $\sim 7 \times 10^{-4}$ M for IR125 and $\sim 1 \times 10^{-3}$ M for IR144.

THEORY

In this section, we use delta function pulses to illustrate the validity of the proposed method. In the perturbation theory of the field-matter interaction, the interaction Hamiltonian operates on the system three times to create a third-order polarizations, $P^{(3)}(t')$. Following three field−matter interactions, one interaction by each pulse, third-order nonlinear signals into the phase-matching directions $\pm\mathbf{k}_1\pm\mathbf{k}_2\pm\mathbf{k}_3$ are generated. In 3PEPS and TG, signals at $-\mathbf{k}_1+\mathbf{k}_2+\mathbf{k}_3$ and/or $\mathbf{k}_1-\mathbf{k}_2+\mathbf{k}_3$ are measured. For resonant interactions of the optical fields with a two-level system, there are eight Liouville space pathways for each of the two phase matching directions.[1,9] In the delta function limit with the time ordering shown in Figure 1, only two Liouville space pathways represented by the Feynman diagrams in Figure 2 are responsible for each signal. For R_1 and R_2, the polarizations during the first coherence period (τ) and that during the second coherence period (t') are complex conjugates of each other to cause rephasing of the polarizations at $t' = \tau$ in the limit of inhomogeneous broadening. In contrast, they are in phase for R_3 and R_4 to lead to the quasi-free induction decay of $P^{(3)}(t')$ vs t'.

Once $M(t)$ or equivalently a spectral density is given, all linear and nonlinear signals can be calculated using the response function formalism via the line broadening function[1]

$$g(t) = i\lambda \int_0^t dt_1\, M(t_1) + \langle \Delta\omega^2 \rangle \int_0^t dt_1 \int_0^{t_1} dt_2\, M(t_2) \quad (3)$$

where λ is a reorganization energy and $\langle \Delta\omega^2 \rangle^{1/2}$ is a coupling strength. The response functions for the four Feynman

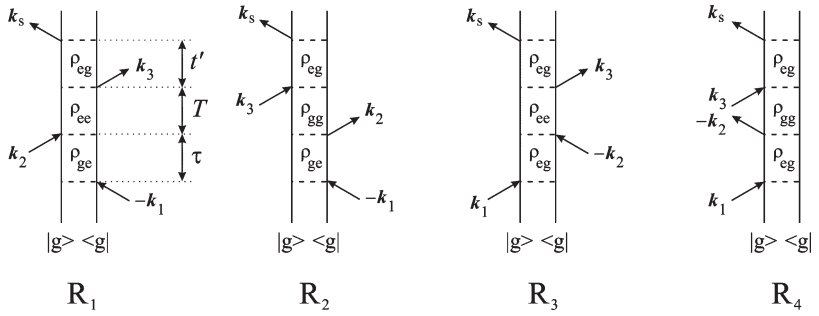

Figure 2. Double-sided Feynman diagrams for the third-order nonlinear polarization into the $-\mathbf{k}_1+\mathbf{k}_2+\mathbf{k}_3$ and $+\mathbf{k}_1-\mathbf{k}_2+\mathbf{k}_3$ phase matching directions for a two-level system $|g\rangle$ and $|e\rangle$. Time ordering of the pulse sequence is given in Figure 1. Four diagrams representing the rephasing (R_1, R_2) and nonrephasing (R_3, R_4) response functions that create population in the excited state and ground state are shown. ρ_{ij} is the nonzero density matrix element for the corresponding time period.

diagrams are[1]

$$R_1 = \exp\{-g^*(\tau) + g(T) - g^*(t') - g^*(\tau+T) - g(T+t') + g^*(\tau+T+t')\} \quad (4a)$$

$$R_2 = \exp\{-g^*(\tau) + g^*(T) - g(t') - g^*(\tau+T) - g^*(T+t') + g^*(\tau+T+t')\} \quad (4b)$$

$$R_3 = \exp\{-g(\tau) - g^*(T) - g^*(t') + g(\tau+T) + g^*(T+t') - g(\tau+T+t')\} \quad (4b)$$

$$R_4 = \exp\{-g(\tau) - g(T) - g(t') + g(\tau+T) + g(T+t') - g(\tau+T+t')\} \quad (4d)$$

For a background-free homodyne detection scheme, the signal at time delays τ and T is given by

$$I(\tau,T) \propto \int_{-\infty}^{\infty} dt' \, |P^{(3)}(\tau,T,t')|^2 \quad (5)$$

In the limit of delta function pulses with the given time ordering, the signals at $-\mathbf{k}_1+\mathbf{k}_2+\mathbf{k}_3$ and $+\mathbf{k}_1-\mathbf{k}_2+\mathbf{k}_3$ represent the rephasing and nonrephasing contributions, respectively:

$$I_R(\tau,T) \propto \int_0^{\infty} dt' \, |R_1 + R_2|^2 \quad (6a)$$

$$I_{NR}(\tau,T) \propto \int_0^{\infty} dt' \, |R_3 + R_4|^2. \quad (6b)$$

In an ordinary TG measurement, where τ is set to zero, a signal into the phase matching direction $-\mathbf{k}_1+\mathbf{k}_2+\mathbf{k}_3$ (or $+\mathbf{k}_1-\mathbf{k}_2+\mathbf{k}_3$) is recorded. Since the rephasing occurs for nonzero τ, a TG signal is not sensitive to the solvation dynamics in the limit of delta function pulses. The sensitivity of a TG (TA) signal on the solvation dynamics arises from the finite pulse duration;[9] nonzero τ values occur through the convolution procedure of finite pulse durations.

A TG signal is sensitive to both solvation dynamics and population relaxation, so that it can be written approximately as a product of the $M(t)$ dependent part and population relaxation. In TRTG, the population period T is scanned while τ is fixed at a finite value. The rephasing signal at $-\mathbf{k}_1+\mathbf{k}_2+\mathbf{k}_3$ can be approximated to be a product of the solvation dynamics contribution and the population relaxation of the excited state, whereas the nonrephasing signal at $+\mathbf{k}_1-\mathbf{k}_2+\mathbf{k}_3$ is regarded lacking the solvation dynamics.

$$I_R(T) \approx \{[f(T) + A_{in}] + C\} \cdot \exp(-2T/\tau_L) \quad (7a)$$

$$I_{NR}(T) \approx C \cdot \exp(-2T/\tau_L) \quad (7b)$$

where $[f(T) + A_m]$ is a function related to the dynamics in $M(t)$ including a constant contribution A_{in} responsible for the inhomogeneity, C is a constant, and τ_L is the excited state lifetime. Therefore, following expression, I_{TRTG}, gives the solvation dynamics including the inhomogeneity, but free from the population relaxation and other processes that erase the transient grating on the sample:

$$I_{TRTG}(T) = \frac{I_R - I_{NR}}{I_{NR}} \quad (8)$$

When the excited state lifetime is much longer than the dynamical time scales in $M(t)$, simple subtraction, $I_{NR} - I_R$, can be used to obtain the solvation dynamics.

In the delta function pulse limit, eqs 4a4 and 6a6 gives

$$I_{R,NR} \propto \int_0^{\infty} dt' \, \exp\{-2[R(\tau) + R(t')]\} \cdot \exp\{\pm 2[R(T) - R(\tau+T) - R(T+t') + R(\tau+T+t')]\} \cos^2[I(T) + I(t') - I(T+t')] \cdot \exp\{-(\tau + 2T + t')/\tau_L\} \quad (9)$$

where the plus and minus signs apply to I_R and I_{NR}, respectively. $R(t)$ and $I(t)$ are the real and imaginary parts of the line broadening function, respectively, and the inhomogeneity of the system is subsumed in $M(t)$. The diffusive dynamics in liquids is usually described by a sum of exponential functions. For a TRTG measurement, τ should be set to a value smaller than or comparable to the electronic dephasing time. This condition arises by considering the τ dependences of I_R and I_{NR}; τ should be kept small because I_{NR} vs τ decays at twice the rate of total electronic dephasing. However, the rephasing process, which differentiates I_R and I_{NR}, occurs for finite τ values. Since the absorption width of a dye in liquid at room temperature is typically on the order of a thousand wavenumbers, the electronic dephasing time is on the order of 10 fs and the polarization

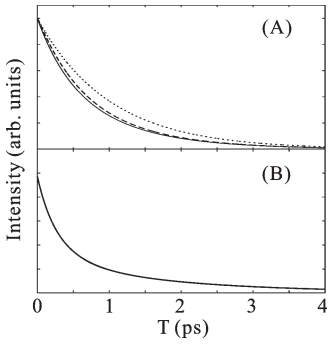

Figure 3. (A) I_{TRTG} (dashed line) vs T calculated by the analytic expression for delta function pulses (eq 14) for a single exponential $M(t)$. Exact calculation (solid line) and the $M(t)$ (dotted line) are shown for comparison. (B) I_{TRTG} calculated by eq 14 for a two exponential $M(t)$ with time constants 400 fs and 2 ps. A two exponential function with the time constants 360 fs and 1.9 ps is overlaid, though indistinguishable.

$P^{(3)}(t')$ decays by the same time scale. For an $M(t) = \exp(-t/\tau_c)$,

$$g(t) = \Delta^2 {\tau_c}^2[\exp(-t/\tau_c) + t/\tau_c - 1] - i\lambda[\exp(-t/\tau_c) - 1] \quad (10)$$

By application of the short time approximation for τ and t', which has been used for the analytic expression of the 3PEPS previously,[15] eq 9 reduces to

$$I_{R,NR} \cong \frac{\sqrt{\pi}}{2\sqrt{\Delta^2 + A^2}} \cdot \exp(-\Delta^2\tau^2) \cdot \exp(-2T/\tau_L) \cdot \exp\left\{\frac{B^2}{4(\Delta^2 + A^2)}\right\} \cdot \left\{1 \pm \mathrm{erf}\left[\frac{B}{2\sqrt{\Delta^2 + A^2}}\right]\right\} \quad (11)$$

where the plus and minus signs correspond to I_R and I_{NR}, respectively, and erf is the error function. A and B are defined as

$$A = \lambda[1 - \exp(-T/\tau_c)] \quad (12a)$$

$$B = 2\Delta^2\tau\exp(-T/\tau_c) \quad (12b)$$

For $M(t)$ with a sum of exponential functions as for a typical liquid, eq 11 is still valid with A, B, and Δ written as a summation

$$A = \sum_i \lambda_i[1 - \exp(-T/\tau_{ci})] \quad (13a)$$

$$B = 2\tau \sum_i {\Delta_i}^2 \exp(-T/\tau_{ci}) \quad (13b)$$

$$\Delta^2 = \sum_i \Delta_i^2 \quad (13c)$$

A TRTG signal by eq 8 becomes

$$I_{TRTG} \cong 2\mathrm{erf}\left[\frac{B}{2\sqrt{\Delta^2 + A^2}}\right] \Big/ \left\{1 - \mathrm{erf}\left[\frac{B}{2\sqrt{\Delta^2 + A^2}}\right]\right\} \quad (14)$$

In an experiment, τ can be made arbitrarily small to make the difference between I_R and I_{NR} small. Then $I_{TRTG}(T)$ is approximately proportional to $M(t)$

$$I_{TRTG}(T) \cong \frac{2\tau M(T)}{\sqrt{\Delta^2 + A^2}} \quad (15)$$

although the denominator is also a function of T as well.

Figure 3A shows $I_{TRTG}(T)$ calculated by eq 14 together with the exact calculation by eq 9 for a single exponential $M(t)$ of time constant 1 ps. The TRTG signal reproduces $M(t)$ very closely, and a nonlinear least-squares fit to a single exponential retrieves the time constant of 0.85 ps. Figure 3B shows I_{TRTG} calculated by eq 14 for an $M(t)$ given by a sum of two exponentials with time constants 400 fs and 2 ps. Again, the TRTG follows $M(t)$ closely, and a nonlinear least-squares fit to a sum of two exponentials retrieves time constants of 360 fs and 1.9 ps.

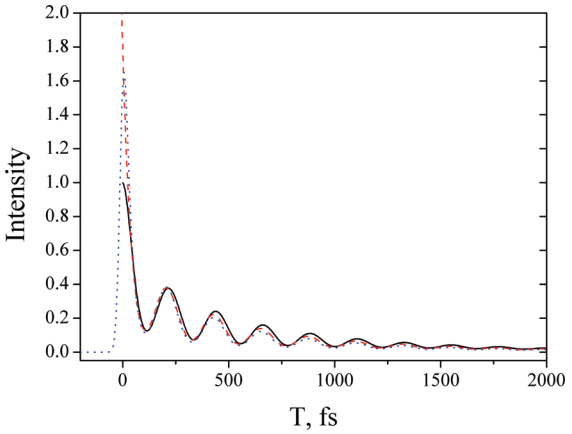

Figure 4. Numerical calculation of I_{TRTG} (red dashed line) and $I_R - I_{NR}$ (blue dotted line) for a model $M(t)$ given in eq 16 considering all response functions and all possible time orderings at 20 fs pulse durations. The two results are nearly the same because the lifetime was set to infinity in these calculation. $M(t)$ (solid line) is also shown for comparison. The parameter values used for calculation as well as the fit results are listed in Table 1.

NUMERICAL SIMULATION

In this section, we establish the validity of the TRTG method by full numerical simulation including finite pulse durations for a realistic model $M(t)$:[19]

$$M(t) = A_1 \cdot \exp[-(t/\tau_1)^2] + A_2 \cdot \exp(-t/\tau_2) + A_3 \cdot \exp(-t/\tau_3) + A_4 \cdot \exp(-t/\tau_4)\cos(\omega_4 t + \phi_4) \quad (16)$$

Here, the Gaussian and two exponential functions reproduce the initial inertial dynamics and solvent dielectric relaxation, respectively, and the damped cosine represents the intramolecular vibrational wave packet motion. I_{TRTG} at τ = 4 fs was calculated for 20 fs input pulses according to the standard procedure described previously. Figure 4 shows the calculated I_{TRTG} together with the $M(t)$. The calculated I_{TRTG} was nonlinear least-squares fitted to the same functional form to judge the conformity between the $M(t)$ and I_{TRTG}. The fit results are listed in Table 1 along with the parameters in $M(t)$, which indicates that the agreement is excellent except the ultrafast Gaussian component. Other nonlinear probes of the solvation dynamics such as 3PEPS, TG, and TA are also known to underestimate the ultrafast time constant and to overestimate the amplitude of the ultrafast component.[9,15] The feature near T = 0 in a TG signal,

Table 1. Parameters in $M(t)$ Used for the Numerical Calculation of I_{TRTG} and the Nonlinear Least Fit Results for the Calculated I_{TRTG} (τ = 4 fs) Using the Same Function[a]

	A_1	τ_1 (fs)	A_2	τ_2 (fs)	A_3	τ_3 (fs)	A_4	τ_4 (fs)	ω_4 (cm^{-1})	ϕ_4 (rad)
$M(t)$	0.39	50	0.24	300	0.15	1000	0.22	500	150	0
I_{TRTG}	0.68	24	0.14	290	0.06	1004	0.12	415	150	0.26
$I_R - I_{NR}$	0.84	16	0.08	249	0.03	944	0.06	370	150	0.22

[a] $I_R(-\mathbf{k}_1+\mathbf{k}_2+\mathbf{k}_3) - I_{NR}(\mathbf{k}_1-\mathbf{k}_2+\mathbf{k}_3)$ are also listed for comparison.

called "coherent spike", becomes stronger as τ increases,[17] which causes the ultrafast decay component of TRTG signal to be faster than that of $M(t)$ and to have larger amplitude. The TRTG signal calculated by subtraction of the nonrephasing signal from the rephasing is also displayed in Figure 4 for comparison. The result from subtraction is, of course, nearly identical to I_{TRTG} by eq 8, because the lifetime is set to infinity in this calculation. Calculations of I_{TRTG} for different pulse durations and detuning from exact-resonance (data not shown) show that I_{TRTG}, when normalized, is mostly insensitive to those parameters to give the solvation dynamics reliably for different experimental conditions, although I_R and I_{NR} are rather sensitive to τ as shown in the experiment (vide infra) and analytic expressions.

EXPERIMENTAL RESULTS AND DISCUSSION

To establish the validity of the TRTG method experimentally, we have performed TRTG measurements for two cyanine dyes IR125 and IR144 dissolved in methanol. Absorption and emission spectra of these dyes are shown in Figure 5. The absorption and the emission spectra of IR125 show mirror symmetry, indicating negligible structural change upon electronic transition, whereas IR144 does not. The Stokes shift of IR144 ($\sim$1500 cm^{-1}) is also much larger than that of IR125 ($\sim$500 cm^{-1}), indicating a large structural change upon electronic transition in IR144, which also implies a relatively large contribution of the intramolecular degrees of freedom on the total Stokes shift. Therefore, IR125 may be more suitable for the study of solvation dynamics, although IR144 has frequently been employed in previous investigations.[9,10,22−24]

A typical TG signal ($\tau = 0$) for a dye molecule in liquid consists of a coherent spike (CS), oscillations due to the wavepacket motion in the ground as well as the exited states, exponential decay corresponding to the dielectric relaxation of solvent, and a slowly decaying large offset due to the population relaxation. Any inhomogeneity that may exist in the system attributable to intramolecular conformational heterogeneity and/or solvent motion slower than population relaxation will be added to the offset. The proportion of each component in a signal may vary with τ. The signals into the $-\mathbf{k}_1+\mathbf{k}_2+\mathbf{k}_3$ direction for several different τ values are shown in Figure 6. As τ increases, CS becomes larger and amplitudes of oscillations and exponential decay increase. At negative τ, which is identical to the $+\mathbf{k}_1-\mathbf{k}_2+\mathbf{k}_3$ signal with positive τ, slowly decaying offset becomes dominant and the oscillation disappears gradually by going further negative τ. This behavior is consistent with our previous result.[17] The τ dependence can be understood easily by considering the response functions with finite pulse duration. Because of the finite pulse duration, the signal into each phase matching direction contains both the rephasing (R_1, R_2) and the nonrephasing (R_3, R_4) contributions. At large τ, however, each

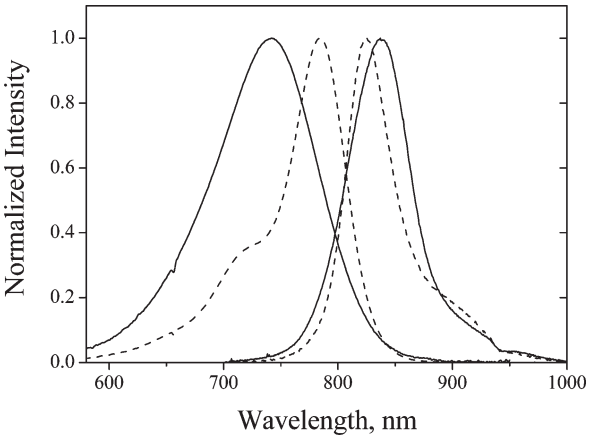

Figure 5. Absorption and emission spectra of IR144 (solid line) and IR125 (dashed line) dissolved in methanol.

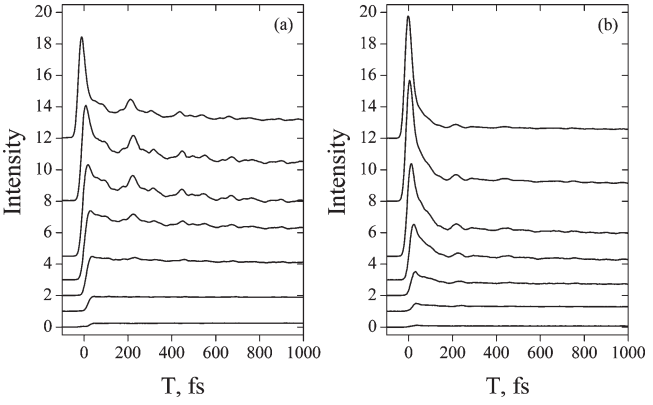

Figure 6. Transient grating signals at several τ values for (a) IR125 and (b) IR144. From top to bottom, τ is set to +24, +16, +8, 0, −8, −16, and −24 fs. Time profiles are arbitrarily displaced vertically.

signal becomes purely rephasing or nonrephasing; that is, the rephasing $-\mathbf{k}_1+\mathbf{k}_2+\mathbf{k}_3$ signal will have more contribution from the dynamics. In addition, when τ is large, the pulse sequence is $\mathbf{k}_1 \rightarrow \mathbf{k}_3 \rightarrow \mathbf{k}_2$ for T smaller than τ.[17] In this situation, it is the coherence period that is actually scanned; that is, a photon echo-like signal is observed for T smaller than τ, and the CS will increase drastically.

We have calculated TRTG signals for several different τ values for the signals shown in Figure 6. When normalized, they give practically the same results excluding the pulse overlap region, although the signal-to-noise ratio (S/N) varies. The optimal delay for τ is determined in such a way that I_{TRTG} is most sensitive to the dynamics in $M(t)$. This occurs at the largest τ to the extent that the rephasing process is largely effective, yet I_{NR} is high enough to give good S/N. In an actual experiment, selecting an optimal τ is ambiguous, because it depends on the pulse duration as well as $M(t)$. We suggest that the τ value in a TRTG experiment can be set roughly to the peak shift value in 3PEPS at $T = 0$.[9] For both IR125 and IR144 solutions, we set τ at 24 fs, and I_R and I_{NR} are measured from −200 fs to 150 ps. The two signals are tail-matched at 150 ps, and I_{NR} is subtracted from I_R. Because the two molecules are laser dyes having lifetimes much longer than 1 ns, $I_R - I_{NR}$ and I_{TRTG} by eq 8 are practically the same. TRTG signals obtained at other τ values show nearly the same decay profile, although CS becomes larger by increasing τ.

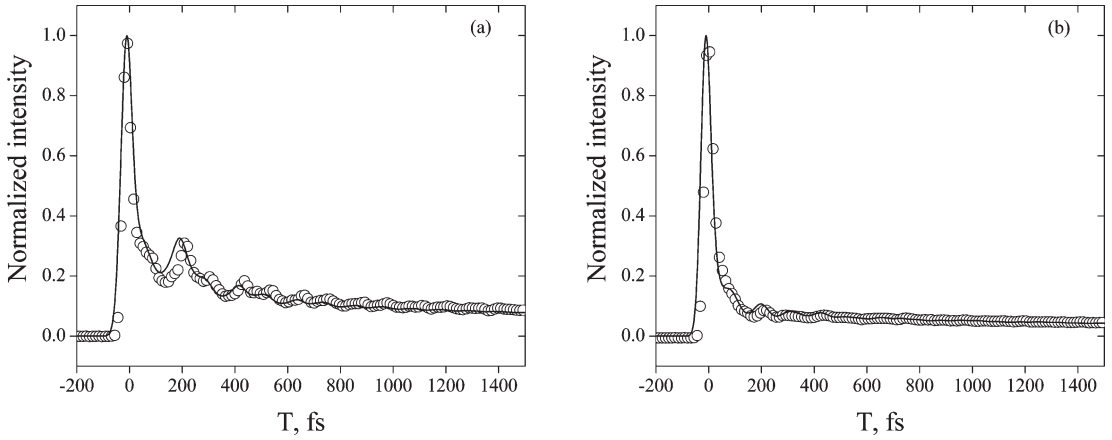

Figure 7. Experimental I_{TRTG} (solid line) of (a) IR125 and (b) IR144 in methanol. Calculated I_{TRTG} (empty circle) for 20 fs pulse duration using the $M(t)$ obtained from the numerical simulation are overlaid as well.

Table 2. Oscillation Frequencies and Dephasing Times for the TRTG Signals of IR125 and IR144 in Methanol Obtained by the Linear Prediction Singular Value Decomposition (LPSVD)

IR125		IR144	
frequency (cm^{-1})	T_2 (fs)	frequency, cm^{-1}	T (fs)
138	190	117	666
302	384	296	127
450	269	446	765
590	647		
737	535		

Table 3. Exponential Fit Results for the TRTG, 3PEPS, and TG for IR125 and IR144 in Methanol

		A_1	τ_1 (fs)	A_2	τ_2 (ps)	A_3	τ_3 (ps)	A_4	τ_4 (ps)
IR125	TRTG	0.64	220	0.24	2.3	0.12	33		
	3PEPS	4.06	287	1.85	3.0	1.14	16		
	TG	0.20	272	0.11	2.4	0.15	11	0.54	126
IR144	TRTG	0.99	30	0.006	1.5	0.004	34		
	3PEPS	7.45	45	1.02	0.8	1.1	6.5		
	TG	0.68	41	0.09	1.2	0.09	10	0.15	189

Figure 7 shows the normalized TRTG signals for IR125 and IR144 in methanol at τ = 24 fs.

We first fit the TRTG signals in the region free from CS (T > 100 fs) by using a linear prediction singular value decomposition (LPSVD) method and Fourier transformation. Frequencies and dephasing times of the oscillations are listed in Table 2. Frequencies of major oscillation are similar to the values reported previously.[2,9] Using the parameters for the oscillation components from LPSVD, TRTG of IR125 and IR144 are fitted to the sum of three exponential functions convoluted with a Gaussian. Results of the exponential fitting of IR125 and IR144 are listed in Table 3. To compare the TRTG with other methods, 3PEPS and TG were also measured by the same apparatus, and the results are also listed in Table 3.

3PEPS of IR125 in methanol was reported to have decay time constants of 250 fs, 1.9 ps, and 16 ps.[2] 3PEPS of IR144 was also reported to have a time constant of 65 fs, 1.4 ps, and 11 ps.[9] The ultrafast and early picosecond decay components of TRTG for IR125 and IR144 are consistent with those of 3PEPS.[2,9,19] Thus, it is entirely clear that TRTG gives the same solvation time constants with 3PEPS without population relaxation contribution. The TG has additional longest decay component corresponding to the population relaxation and rotational diffusion as the polarizations of the pulses are all parallel.

Although TRTG itself follows $M(t)$ closely, theory showed that TRTG is not exactly the same as $M(t)$. Moreover, the effect of finite pulse duration may affect the signal as well. Here, we use eq 16 as a model $M(t)$ to generate a TRTG signal by full numerical simulation and compare with the experiment to determine the $M(t)$ that generate the experimentally observed TRTG. Once $M(t)$ is determined, all linear and nonlinear spectroscopic signals can be calculated from it. The calculated TRTG signals using the $M(t)$ thus obtained are also shown in Figure 7. The calculated and measured signals match closely, demonstrating the soundness of the TRTG method. In addition, the $M(t)$ also gives an absorption that closely matches the experimental absorption spectra (data not shown).

One attractive feature of 3PEPS is its unique capability to pick out a static (inhomogeneous) component in $M(t)$ on the time scale of the measurement,[19] which is the lifetime of the probe molecule. In principle, TRTG given by eq 8 can also give such information, provided that relative intensities of the two signals at $-\mathbf{k}_1+\mathbf{k}_2+\mathbf{k}_3$ and $\mathbf{k}_1-\mathbf{k}_2+\mathbf{k}_3$ are measured accurately. In practice, however, this may not be feasible, and we used the tail-matching method at 150 ps, which removes the information on the dynamics in $M(t)$ slower than 150 ps. We note, however, that it might be possible to obtain such information by employing a reference probe, where inhomogeneity is not present. That is, sensitivities of the two detection channels may be obtained by assuming their intensities to be the same at long times.

By a quick look at the TRTG of the two dyes, differences are readily discernible as expected from the steady state spectra and the TG results in Figure 6. In particular, CS in IR144 is much larger than that in IR125. In the case of IR144, the signal shows ultrafast decay at early times and oscillations with small amplitude are over before 1 ps, whereas the signals of IR125 decay slowly and maintain large oscillations over 1 ps. In the electronic ground state, IR144 and IR125 have resonance structures and large dipole moments.[22,25] Upon electronic excitation, the dipole

moment of IR144 reduces instantaneously[22] and its structure evolves significantly,[26] whereas IR125 is expected not to change much in dipole moment. As a result, IR144 and IR125 go through polar solvation and nonpolar solvation, respectively. A similar result was reported in solvation dynamics study of xanthene and styryl dyes by 3PEPS measurements, where styryl dyes with large Stokes shift show polar solvation and rapid decay in 3PEPS signals.[27]

CONCLUSION

We have developed a four wave mixing scheme, τ-resolved transient grating (TRTG), that gives dynamical information similar to the 3PEPS and transient grating with several advantages. This method is based on the TG method, but as in 3PEPS it is free from the population relaxation and other dynamics that reduces the intensity of a TG signal. We achieved this by setting the electronic coherence time delay at some small value to an interferometric accuracy and measuring the rephasing and nonrephasing contributions to the TG signal separately and simultaneously. It is shown by theory and experiment that a TRTG signal follows directly the transition frequency correlation function $M(t)$. For delta function pulses, an analytic expression for TRTG in terms of $M(t)$ is obtained. We have also performed full numerical calculation for a realistic $M(t)$ including finite pulse duration to show the conformity between the TRTG and $M(t)$. TRTG has also been demonstrated experimentally for two cyanine dyes IR144 and IR125 dissolved in methanol by using a diffractive-optics based three pulse four wave mixing apparatus. The solvation dynamics obtained by TRTG are consistent with the values reported previously by 3PEPS and TG and the values measured in this work using the diffractive optics. Solvation dynamics of the two molecules IR125 and IR144 are differen,t representing the nonpolar and polar solvation dynamics, respectively, due to the magnitude of the dipole moment change upon electronic transition.

AUTHOR INFORMATION

Corresponding Author

*E-mail: thjoo@postech.ac.kr. Fax: +82-54-279-8127.

Present Addresses

[†]Samsung Electro-mechanics Co. LTD, Suwon, 443-743, Korea

ACKNOWLEDGMENT

This work was supported by the National Research Foundation of Korea (NRF) grant funded by the Korea government (MEST) (2010-0001634) and in part by the Midcareer Researcher Program (2010-0000500).

REFERENCES

(1) Mukamel, S. *Principles of Nonlinear Optical Spectroscopy*; Oxford University Press: New York, 1999.
(2) Park, J. S.; Joo, T. *J. Chem. Phys.* **2002**, *116*, 10801.
(3) Horng, M. L.; Gardecki, J. A.; Papazyan, A.; Maroncelli, M. *J. Phys. Chem.* **1995**, *99*, 17311.
(4) Eom, I.; Joo, T. *J. Chem. Phys.* **2009**, *131*, 244507.
(5) Yarwood, J.; Catlow, B. *J. Chem. Soc., Faraday Trans. 2* **1987**, *83*, 1801.
(6) Tassaing, T.; Danten, Y.; Besnard, M.; Zoidis, E.; Yarwood, J. *Chem. Phys.* **1994**, *184*, 225.
(7) Walker, S.; Jain, S. R. *J. Phys. Chem.* **1971**, *75*, 2942.
(8) Bagchi, B.; Oxtoby, D. W.; Fleming, G. R. *Chem. Phys.* **1984**, *86*, 257.
(9) Joo, T.; Jia, Y. W.; Yu, J. Y.; Lang, M. J.; Fleming, G. R. *J. Chem. Phys.* **1996**, *104*, 6089.
(10) Nagasawa, Y.; Yu, J. Y.; Fleming, G. R. *J. Chem. Phys.* **1998**, *109*, 6175.
(11) Farrow, D. A.; Yu, A.; Jonas, D. M. *J. Chem. Phys.* **2003**, *118*, 9348.
(12) Nagasawa, Y.; Seike, K.; Muromoto, T.; Okada, T. *J. Phys. Chem. A* **2003**, *107*, 2431.
(13) Pshenichnikov, M. S.; Duppen, K.; Wiersma, D. A. *Phys. Rev. Lett.* **1995**, *74*, 674.
(14) deBoeij, W. P.; Pshenichnikov, M. S.; Wiersma, D. A. *Chem. Phys. Lett.* **1996**, *253*, 53.
(15) Cho, M. H.; Yu, J. Y.; Joo, T.; Nagasawa, Y.; Passino, S. A.; Fleming, G. R. *J. Phys. Chem.* **1996**, *100*, 11944.
(16) Xu, Q. H.; Scholes, G. D.; Yang, M.; Fleming, G. R. *J. Phys. Chem. A* **1999**, *103*, 10348.
(17) Park, J. S.; Joo, T. *J. Chem. Phys.* **2004**, *120*, 5269.
(18) Joo, T.; Albrecht, A. C. *Chem. Phys.* **1993**, *176*, 233.
(19) Park, S.; Joo, T. *J. Chem. Phys.* **2009**, *131*, 164508.
(20) Maznev, A. A.; Crimmins, T. F.; Nelson, K. A. *Opt. Lett.* **1998**, *23*, 1378.
(21) Goodno, G. D.; Dadusc, G.; Miller, R. J. D. *J. Opt. Soc. Am. B* **1998**, *15*, 1791.
(22) Yu, A. C.; Tolbert, C. A.; Farrow, D. A.; Jonas, D. M. *J. Phys. Chem. A* **2002**, *106*, 9407.
(23) Hybl, J. D.; Ferro, A. A.; Jonas, D. M. *J. Chem. Phys.* **2001**, *115*, 6606.
(24) Passino, S. A.; Nagasawa, Y.; Fleming, G. R. *J. Chem. Phys.* **1997**, *107*, 6094.
(25) Bertolino, C. A.; Ferrari, A. M.; Barolo, C.; Viscardi, G.; Caputo, G.; Coluccia, S. *Chem. Phys.* **2006**, *330*, 52.
(26) Carson, E. A.; Diffey, W. M.; Shelly, K. R.; Lampa-Pastirk, S.; Dillman, K. L.; Schleicher, J. M.; Beck, W. F. *J. Phys. Chem. A* **2004**, *108*, 1489.
(27) Nagasawa, Y.; Watanabe, A.; Takikawa, H.; Okada, T. *J. Phys. Chem. A* **2003**, *107*, 632.